Modeling of thermal transient processes in frequency-controlled induction motor

Yavor LOZANOV, Svetlana TZVETKOVA and Angel PETLESHKOV
Department of Electrical Supply, Electrical Equipment and Electrical Transport
Technical University of Sofia
Sofia, Bulgaria
E-mail: ylozanov@tu-sofia.bg, stzvet@tu-sofia.bg, apetl@tu-sofia.bg

***Abstract* — The paper presents a model of thermal transients in induction motor controlled via a variable frequency drive, which takes into account the operation of the motor at speeds different than the rated one. Experimental recording of motor heating curves at different angular speeds has been done, to verify the model.**

Keywords — adjustable speed drive, heating curves, induction motor, thermal transients.

I. INTRODUCTION

The most widely used electric motor in all areas of the industry is the squirrel cage induction motor. The reason for this is the relatively simple design of this type of motor, which provides easier maintenance and lower costs and good operational performance of the machine.

As with every element of the electrical equipment, a large number of failures occur in the induction motors. Early diagnosis of these faults prevents financial losses and unplanned downtime on production lines. Electric drives failures are often preceded by a considerable period of working with the higher temperature rise of the various components of the system. In case of timely detection of the temperature rise, it is possible to take measures to improve the technical condition of the elements of the drive and to prevent possible sudden failures. As a result, temperature can be a key parameter for monitoring and controlling technological processes, for monitoring and controlling the technical condition and diagnostics of machine malfunctions.

Information on the technical condition of the machines understudy can be obtained from the thermographic images in steady-state temperature mode as well as from a series of thermographic images obtained in dynamic temperature regimes (thermal transients). In practice, heating and cooling curves of electric motors are used as criteria for evaluating their technical condition [1,2].

II. THERMAL MODEL OF THE INDUCTION MOTOR

The thermal transients that occur in induction motors are phenomena of complex description. The reason for this is that the induction motor is a heterogeneous body whose elements are made of different structural materials (copper, aluminum, steel, insulation, etc.) [1, 3, 7].

In its foundation, the thermal models of the induction motor are based on the balance of energy losses in the machine:

$$m_m C_{m\,eq} \frac{dT}{dt} = \Delta P - q_{tot}\,, \qquad (1)$$

where: m_m is the mass of the motor;

$C_{m\,eq}$ - equivalent specific heat capacity of the elements of the motor;

ΔP - power losses in the motor;

q_{tot} - total heat dissipation from the motor.

In totally enclosed type motors, the total heat output is dissipated in the environment mainly by natural and forced convection, and by radiation:

$$q_{tot} = q_{n\,conv} + q_{f\,conv} + q_{rad}\,, \qquad (2)$$

where: $q_{n\,conv}$ is the heat transfer rate through natural convection;

$q_{f\,conv}$ - heat transfer rate through forced convection;

q_{rad} - heat transfer rate through radiation, the value of which can be calculated according to the Stefan-Boltzmann law [4].

The heat transfer rate by natural convection can be determined by Newton's law of heating and cooling of bodies:

$$q_{n\,conv} = h_{nat} S (T_S - T_{amb})\,, \qquad (3)$$

where: h_{nat} is the natural convection heat transfer coefficient;

S - area through which the heat exchange takes place;

T_{amb} - ambient temperature;

T_S - object's surface temperature.

Research and Development Sector at the Technical University of Sofia.

978-1-7281-4346-0/20/$31.00 ©2020 IEEE

The natural convection heat transfer coefficient of a body with complex geometry, such as the induction motor, can be determined experimentally using the cooling curve of the motor taken at standstill condition. At standstill, of the motor, the heat exchange with the environment is carried out only by radiation and natural convection. The first step in determining the natural convection heat transfer coefficient is to calculate the total heat energy that is dissipated into the environment during the cooling process. The next step is the determination of the amount of heat energy dissipated by radiation. The amount of heat energy dissipated due to natural convection $Q_{n\,conv}$ is defined as the difference between the total heat energy output during the cooling process and the heat energy dissipated by radiation. Taking this into account the natural convection heat transfer coefficient is determined by the dependence:

$$h_{nat} = \frac{Q_{n\,conv}}{S(T_S - T_{amb})t}, \qquad (4)$$

where: t is the duration of the transient process.

In self-ventilation asynchronous motors, the forced convection heat transfer coefficient depends on the design features of the machine and on the air velocity in the ventilation channels of the motor. The latter changes significantly when the motor speed changes. It follows that in the case of adjustable speed drives with wide speed control ranges, a change in the dynamic thermal behavior of the motor will be observed. In totally enclosed, fan cooled (TEFC) motors, forced convection heat transfer causes improved power losses dissipation compared to equivalent natural ventilated (TENV) machines [5].

The housing of the totally enclosed fan cooled motors (TEFC) is usually ribbed in order to increase the area for convective heat transfer. In addition, in most TEFC motors, the ventilation channels are semi-open, which does not allow the direct use of expressions for aerodynamic and thermal processes. In these cases an empirical formula for semi-open channels is used. The formula was obtained based on extensive research on the housings of induction motors of different sizes and shapes. The forced convection heat transfer coefficient is calculated using the following equation:

$$h_f = \frac{\rho c_p D v}{4L}.(1 - e^{-m}), \qquad (5)$$

where: v is the air velocity at the inlet side of the ventilation channel;

D - hydraulic diameter (four times cross-sectional area of the channel divided by the perimeter of the channel);

L – length of the ventilation channels;

ρ and c_p are the density and specific heat capacity of air.

The determination of the exponent m is performed according to the following formula:

$$m = 0.1448 \frac{L^{0.946}}{D^{1.16}}.\left(\frac{k}{\rho c_p v}\right)^{0.214}, \qquad (6)$$

where: k is the fluid (air) thermal conductivity.

For these formulae, it is assumed that the air-flow is always turbulent due to the fact that the axial fans and cowlings used in such machines create turbulence. Experimental studies have shown that the value of forced convection heat transfer coefficient obtained by (5) must be multiplied by the coefficient of turbulence, which has values between 1.7 and 1.9 and does not depend on the air velocity in the ventilation channels [6].

The coefficient of convection heat exchange by mixed convection is defined as:

$$h_{mix}^3 = h_f^3 \pm h_{nat}^3 . \qquad (7)$$

The sign in the upper equation is determined by the direction of movement of the air flows, sign + for co-directional or perpendicular flows, and the sign - for opposite directions.

The change of temperature of the motor housing over time can be obtained by converting (1) to the following form:

$$\frac{dT}{dt} = \frac{1}{m_m C_{m\,eq}}[\Delta P(t) - (q_{n\,conv}(t) + q_{f\,conv}(t) + q_{rad}(t))] \qquad (8)$$

The numerical solution of the differential equation under the initial conditions obtained from thermographic measurements and reading of electrical quantities represents the model (the theoretical heating curve).

III. Characteristics of the Object of Research

The object of research is an adjustable electric drive with a three-phase, squirrel cage rotor induction motor. The motor is four-pole with a rated power of 0,37 kW, and the motor housing is made of aluminum. The variable-frequency drive has a power of 0,75 kW and allows adjusting the motor's speed in the range from 160 to 2000 rpm.

Temperature measurements are performed with a FLIR E60 thermal imaging camera controlled by a personal computer, which allows recording the development of transients. The duration of the measurement when recording the heating curve is 40 min and the temperature values are read every 0.13 s. The required electrical quantities are measured with measuring devices allowing connection to the thermal imaging camera and recording of the readings of the devices. A thermo-anemometer is used to determine the non-electrical quantities -

ambient temperature and air velocity in the ventilation channels of the motor.

Motor temperature measurements during transients are performed when the motor is running idle at different angular speeds. The idling mode is used in view of the possibility to directly determine the power losses in the motor ΔP. The selection of the motor's rated power is consistent with the ratio of the magnitude of losses in the motor to its rated power, which is large for low-power motors.

When measuring the air velocity, in order to eliminate the influence of the electromagnetic field of the motor on the thermo-anemometer, a remote diffuser is used. The diameter of the orifice of the diffuser at the point of measurement of the air velocity is $d = 30mm$. This method of measurement allows obtaining only the volumetric flow rate passing through the motor fan. To obtain the air-flow distribution in the machine and the values of the air velocity in the ventilation channels, a 3D model of the motor was developed and simulations were performed. The results of the simulations of the air-flow in the machine at the minimum and maximum rpm are presented in Fig.1 and Fig.2, respectively.

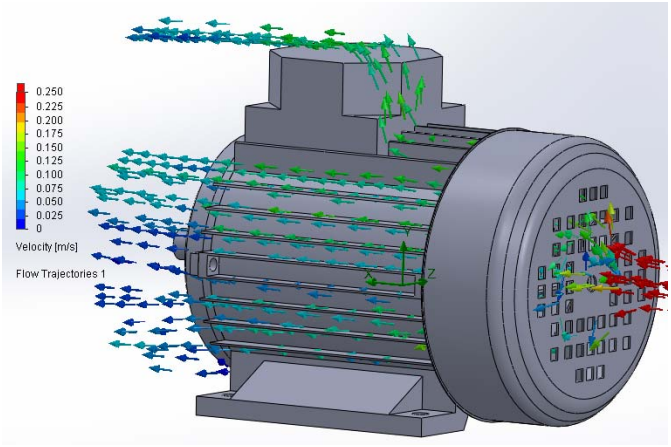

Fig. 1. Air- flow distribution in the IM at 160rpm.

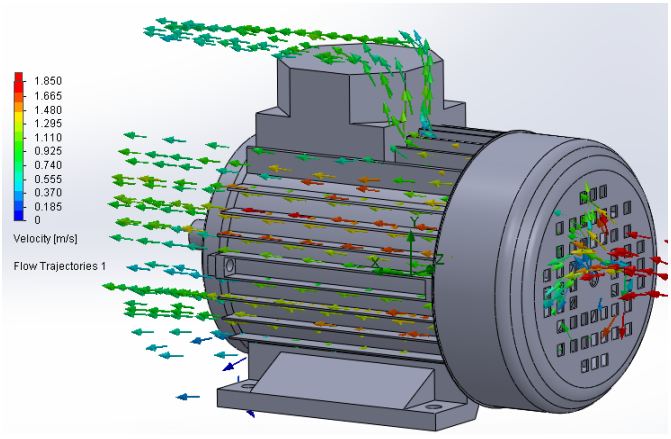

Fig. 2. Air- flow distribution in the IM at 2000rpm.

The developed accurate 3D model of the motor also allows to easily obtain the area of the surrounding surfaces and the mass of the individual elements of the motor. These parameters are needed for the modeling of the processes of heat exchange and heating (cooling) of the motor. The results for the area of the surrounding surfaces of the individual engine components are shown in Table 1.

TABLE I. OUTER SURFACES OF MOTOR ELEMENTS

Element	Surface S, m^2
Motor frame	
Frame cylinder	0,06
Fins	0,056
Legs	0,0244
Bearing shields	
Drive end bearing shield	0,0178
Non-drive end bearing shield	0,0178
Other elements	
Shaft drive end	0,002
Terminal box - fixed part	0,008
Total surface	0,186

The total mass of the elements of the housing through which the heat exchange with the environment takes place is $m_{mh} = 0{,}982kg$, and the value of the specific heat capacity of the material from which the engine housing is made is $C_{mh} = 897J/kg.K$.

The masses of the stator elements are magnetic core $m_{st\,c} = 2{,}1kg$ and winding $m_{st\,arm} = 0{,}55kg$, respectively. The values of the specific heat capacity of the stator materials are $C_{st\,c} = 463\,J/kg.K$ and $C_{st\,arm} = 385\,J/kg.K$.

IV. RESULTS AND ANALYSIS OF THERMAL PROCESSES IN THE INDUCTION MOTOR

For each of the set values of the rotational speed, the volume flow rate of the air passing through the motor fan has been measured and the air velocity in the ventilation channels of the motor is obtained by simulation. Based on the received velocities of the air-flow in the ventilation channels, the values of the forced convection heat transfer coefficient are calculated. The results of the measurements, simulations, and calculations are presented in Table 2.

TABLE II. RESULTS FOR THE AIR VELOCITY

n, min^{-1}	$v_{in\text{-}d30}$, m/s	$q_{in\text{-}d30}$, m^3/s	v_{chan}, m/s	h_f, W/m^2K
161	0,7	4,948E-06	0,084	13,472
300	1,3	9,189E-06	0,177	16,820
500	2,1	1,484E-05	0,368	18,798
700	2,9	2,050E-05	0,565	19,505
900	3,8	2,686E-05	0,765	19,864
1100	4,4	3,110E-05	0,919	20,036
1300	5,1	3,605E-05	1,118	20,191
1500	6,1	4,312E-05	1,302	20,292
1700	6,7	4,736E-05	1,477	20,366
2000	7,7	5,443E-05	1,667	20,429

The graphical presentation of the change in the air velocity in the ventilation channels of the motor depending on the rotational speed is shown in Fig.3

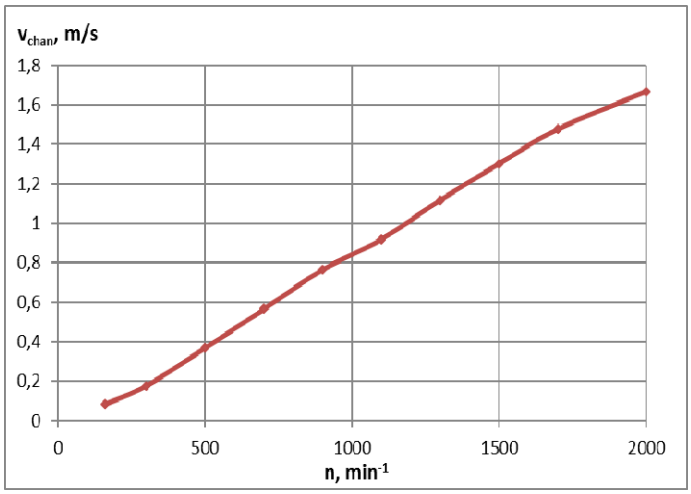

Fig. 3. Dependence of air-flow velocity in ventilation channels from motor's rpm.

The change of the forced convection heat transfer coefficient depending on the motor speed is shown in Fig.4. It shows that when the speed decreases, the value of the forced convection heat transfer coefficient remains relatively unchanged up to about 700min^{-1}, after which it begins to decrease rapidly.

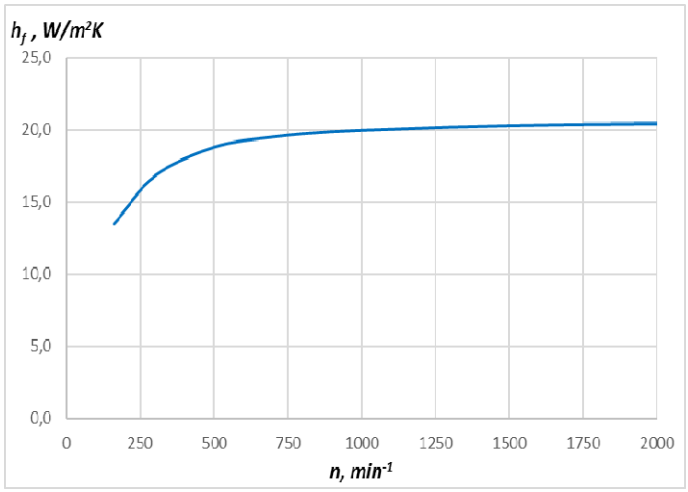

Fig. 4. Dependence of forced convection heat transfer coefficient from motor's rpm.

The value of the natural convection heat transfer coefficient is $h_{nat} = 4{,}149$ and is obtained experimentally from the motor cooling curve.

During the study, the values of the electrical quantities - linear voltage, current, and real power have been measured, for each of the set values of the rotational speed. The values of the measured and calculated electrical quantities are shown in Table 3.

TABLE III. RESULTS FROM THE MEASUREMENT OF ELECTRICAL QUANTITIES

n,min^{-1}	*U_{ph-ph}, V*	*I_{avg}, A*	*P, W*	*S, VA*	*cosφ*
161	83,6	0,780	67	112,9	0,593
300	106,7	0,777	71	143,5	0,495
500	175,1	0,773	76	234,5	0,324
700	237,2	0,723	83	297,2	0,279
900	308,4	0,687	91	366,8	0,248
1100	340,6	0,630	99	371,7	0,266
1300	344,0	0,503	108	299,9	0,360
1500	344,8	0,450	118	268,7	0,439
1700	345,1	0,393	129	235,1	0,549
2000	347,3	0,370	147	222,6	0,660

Fig. 5 shows the change of the power consumed by the motor (power losses) at different rotational speeds.

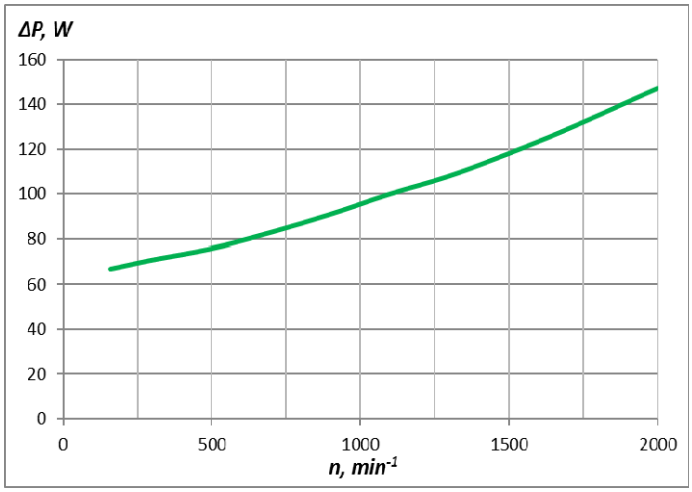

Fig. 5. Change of the power consumed at different rpm.

When capturing the motor heating curve, the results are obtained both in the form of a series of thermographic images and by directly depicting the change in temperature reading from a given thermographic measurement tool.

The thermographic image of the studied motor at the end of the thermal transient process and the motor's heating curve drawn for the highest measured temperature are shown in

Fig.6. The presented thermographic image and heating curve are obtained when operating the motor at a rotational speed of 1300min^{-1}. Periodically occurring stepped changes in the captured heating curve are due to the processes of recalibration of the thermal imaging camera during operation. The large values of noise (deviation of the measured temperature) at the beginning of the thermal transient process are due to the influence of the reflected temperature on the accuracy of the temperature readings.

After recording the motor heating curve, the obtained data is imported into MATLAB for further processing. Based on the obtained temperature values, the heat transfer rates by radiation, and natural and forced convection during the transient process is calculated. The results of the calculations of the individual heat transfer rates are presented in Fig.7.

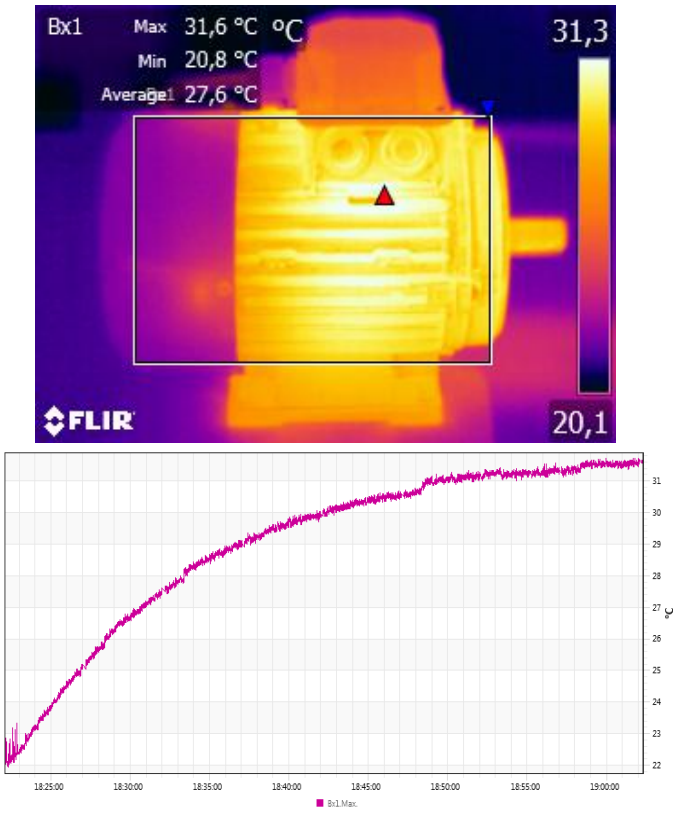

Fig. 6. Thermographic image of the motor at end of the heating transient process and corresponding heating curve.

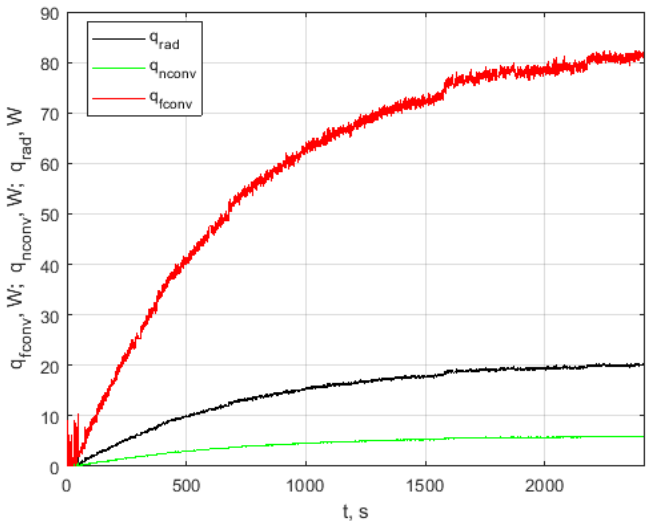

Fig. 7. Change of the heat transfer rates through radiation, and natural and forced convection in time.

Once all the elements of the model (8) and the initial conditions are known, proceeds to determine the theoretical value of the temperature of the motor housing and its change over time - obtaining a theoretical heating curve. The results of the modeling of the theoretical motor heating curve when operating at 1300 min^{-1} are shown in Fig.8.

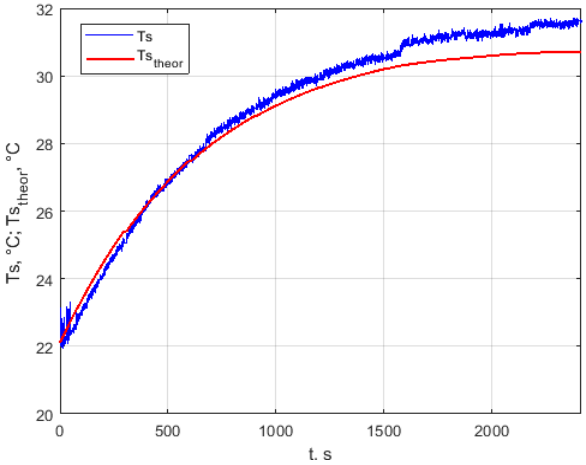

Fig. 8. Theoretical heating curve of the motor.

It can be seen from Fig. 8 that the model thus defined provides a sufficiently accurate description of the thermal processes in the motor, by means of input data which can be easily measured during the operation of the machine. A further increase in the accuracy of the model would be possible by developing a methodology for accurately determining the turbulence coefficient, the value of which in this case is assumed to be 1,8. Another factor that would increase the accuracy of the model is the appropriate choice of the parameters of the thermal imaging camera.

CONCLUSION

The considered model of thermal processes takes into account the operation under variable cooling conditions. The

model is applicable to fully enclosed self-ventilated motors with different configurations.

The model is based on values that can be easily determined during operation without disturbing the normal operation of the technological units.

The comparison of the modeled and measured heating curves of the motor can be applied as criteria for assessment of its technical condition when performing thermographic diagnostics.

It is possible to increase the accuracy of the model by establishing a relationship between the turbulence coefficient and the design characteristics of the machine.

ACKNOWLEDGMENT

The authors would like to thank the Research and Development Sector at the Technical University of Sofia for the financial support.

REFERENCES

[1] A. Boglietti, A. Cavagnino, David Staton. Evolution and modern approaches for thermal analysis of electrical machines, IEEE Transactions on Industrial Electronics Volume: 56, Issue: 3, 2009, pp. 871 – 882, DOI: 10.1109/TIE.2008.2011622.

[2] M. Narrol, W. Stiver. Quantitative thermography for electic motor efficienty diagnosis, Home / Archives / 2005: Proceedings of the Canadian Design Engineering Network (CDEN) Conference, 2005, DOI: 10.24908/pceea.v0i0.3947.

[3] J. Nunez, L. Velazquez, L. Morales-Hernández, R. Osornio-Rios. Low-cost thermographic analysis for bearing fault detection on induction motors, Journal of scientific and industrial research Vol.75 Issue, 2016, pp.412-415.

[4] M.J. Picazo-Ródenas, R. Royo, J. Antonino-Daviu, J. Roger-Folch. Energy balance and heating curves of electric motors based on infrared thermography, 2011 IEEE International Symposium on Industrial Electronics, 2011, DOI: 10.1109/ISIE.2011.5984224.

[5] M. A. Valenzuela, J. Tapia, J. A. Rooks. Thermal evaluation of tefc induction motors operating on frequency-controlled variable-speed drives, IEEE Transactions on industry applications, vol. 40, no. 2, March/April 2004, pp 692-698.

[6] D.A. Staton, A. Cavagnino. Convection heat transfer and flow calculations suitable for electric machines thermal models, IEEE Transactions on industrial electronics, vol. 55, no. 10, October 2008.

[7] F. Ferreira, A. de Almeida, J. Carvalho, M. V. Experiments to observe the impact of power quality and voltage-source inverters on the temperature of three-phase cage induction motors using an infra-red camera, 2009 IEEE International Electric Machines and Drives Conference, 2009, DOI: 10.1109/IEMDC.2009.5075373.